PROTON NUCLEAR SCATTERING RADIOGRAPHY

J.C. Duchazeaubeneix, J.C. Faivre, D. Garreta, B. Guillerminet, D. Legrand, M. Rouger, J. Saudinos
DPh-N/ME, CEN Saclay, 91191 Gif-sur-Yvette Cedex, France

and

G. Charpak, G. Melchart, Y. Perrin, J.C. Santiard, F. Sauli
CERN, Geneva, Switzerland

Nuclear scattering of protons allows to radiograph objects with specific properties : direct 3- dimensional radiography, different information as compared to X-ray technique, hydrogen radiography. Furthermore, it is a well adapted method to gating techniques allowing the radiography of fast periodic moving systems. Results obtained on different objects (light and heavy materials) are shown and discussed. The dose delivery is compatible with clinical use, but at the moment, the irradiation time is too long between 1 and 4 hours. Perspectives to make the radiography faster and to get a practical method are discussed.

Introduction

Nuclear scattering radiography (N.S.R.) relies to strong nuclear interaction.[1-3] When protons in the GeV energy range are incident on an object, most of them go through with a very small angular deviation due to multiple Coulomb scattering (M.C.S.) and a little energy loss. Some of the particles, however, have strong nuclear interactions with the nucleons bound in the nuclei of the atoms of object. The collision called quasi-elastic has nearly the character of an elastic encounter between particles of the same mass ; so the angular deviation of the incident particle is big. Practically the useful range is 15-40°. Measuring the trajectories of the incoming and outgoing charged particles, one may compute the three space coordinates of the interaction vertices whose density distribution reflects the matter distribution in the bombarded body. So one obtains directly 3-D radiography without moving the incident beam or the object. The number of protons scattered by a volume element is directly proportional to the nuclear quasi-elastic cross section. Its dependence on the atomic mass A is very different from that of X-ray coefficients : in case of N.S.R., interaction, lengths are higher and this makes possible the radiography of thicker or heavier materials. Radiograpns obtained by measuring only the incident and scattered trajectories are called simple radiographs by opposition to the hydrogen radiographs obtained by observing a third particle, the recoil nucleon. In that case, kinematical relations between the three particles allow to separate the nuclear scattering on hydrogen atoms from scattering on all other elements. It gives an information on the hydrogen content of targets.

Experimental method

The experimental set-up consists mainly of four multiwire proportional chambers CH (planes X-Y) perpendicular to the beam direction (Z-axis). CH_1 and CH_2 placed before the target localize the incident particle (coordinates X_1Y_1, X_2Y_2). Their useful area which defines the field of radiography is 20 × 20 cm² and their localization resolution is 0.6 mm. CH_3 and CH_4 placed after the target localize the scattered proton (coordinates X_3Y_3, X_4Y_4) up to a scattering angle of 40° : their useful area is 100 × 100 cm² and their localization resolution between 1 and 2 mm. CH_3 is able also to localize a recoil proton if any (coordinates X_5Y_5). A coding system reads the eight or ten coordinates and transfers them to a fast computer called SAR.[4] It takes less than 2 µs for this operation. SAR computes the coordinates $X_RY_RZ_R$ of the intersection in space of the incident and scattered straight lines defined by X_1Y_1, X_2Y_2 and X_3Y_3, X_4Y_4. SAR is directly coupled to a mass memory of 2.1 millions of 12 bits elements. This memory is used as a three-dimensional matrix X,Y,Z, typical dimensions being 160 , 160 , 80. Each element of the mass memory corresponds to an elementary volume (voxel) of the target defined by : $\Delta V = \Delta X \times \Delta Y \times \Delta Z$. ΔX, ΔY, ΔZ are chosen in function of the localization resolution of the system. Typical values are 0.635 or 1.27 mm for ΔX and ΔY, 2.54 or 5.08 mm for ΔZ. When one event satisfies the conditions $X \leq XR < X + \Delta X$, $Y \leq YR < Y + \Delta Y$, $Z \leq ZR < Z + \Delta Z$, SAR adds one count to the voxel of address X, Y, Z. All of these operations take about 50 µs to be completed. In case of hydrogen radiography, SAR has also to compute two kinematical criteria and it takes 100 µs to analyze one event. Because the duty cycle of the SATURNE accelerator in Saclay, we are presently able to measure about then thousands scattered events per second in case of simple radiography. With this acquisition rate, after an irradiation of four hours, the mass memory contains about one hundred millions of scattered events. For each voxel, the number of events is proportional to the density and to the nuclear cross sections of the corresponding target voxel. The 3D-matrix is stored on a magnetic tape and has to be corrected for various parasitic effects : lack of uniformity of the incident beam, variations of the solid angle of detection, differential absorption of particles in large targets. It is possible also by smoothing techniques to decrease the statistical fluctuations and to improve the sensitivity at the cost of a loss in spatial resolution. To visualize the 3-D matrix on a T.V. set, one shows successions of adjacent slices in three orthogonal planes : perpendicular to the beam (slice X-Y), vertical parallel to the beam (slice ZY) or horizontal (slice ZX). A gray scale is used with the highest pixel value being white and the lowest black. To increase the contrast of the radiographs, one may subtract a constant quantity.

A detailed description of the method can be found elsewhere.[5]

Experimental results

We present different results to illustrate possible applications in technology and medicine.

I. Detection and localization of defects in heavy materials

Taking advantage of the relatively small nuclear absorption involved in N.S.R., we have looked at the limits of defect detection and localization in metals like iron, copper, lead,uranium.[6] Defects are plane air gaps between metal blocks, perpendicular to the beam axis. The gap width may be varied. In that conditions, for iron we detected and localized defects of 0.1, 0.2 and 0.4 mm width in blocks of thickness 4, 11 and 22 cm respectively. For the thicker blocks the limitation comes from errors given by M.C.S. It could be improved by increasing the energy of the incident proton.

II. Radiography of an electric motor

To illustrate the capability of N.S.R. in technical application, Fig. 1 shows the radiography of an electric motor at rest.

Motor diameter is 10 cm, its length 20 cm. The motor axis is along the proton beam direction (Z-axis). The visualization matrix M(X,Y,Z) has dimensions 160 , 160 , 80 respectively and $\Delta X = \Delta Y = 0.635$ mm, $\Delta Z = 2.54$ mm

Nuclear science symposium
Washington, USA 20 - 22 Oct 1982
CEA-CONF--6561

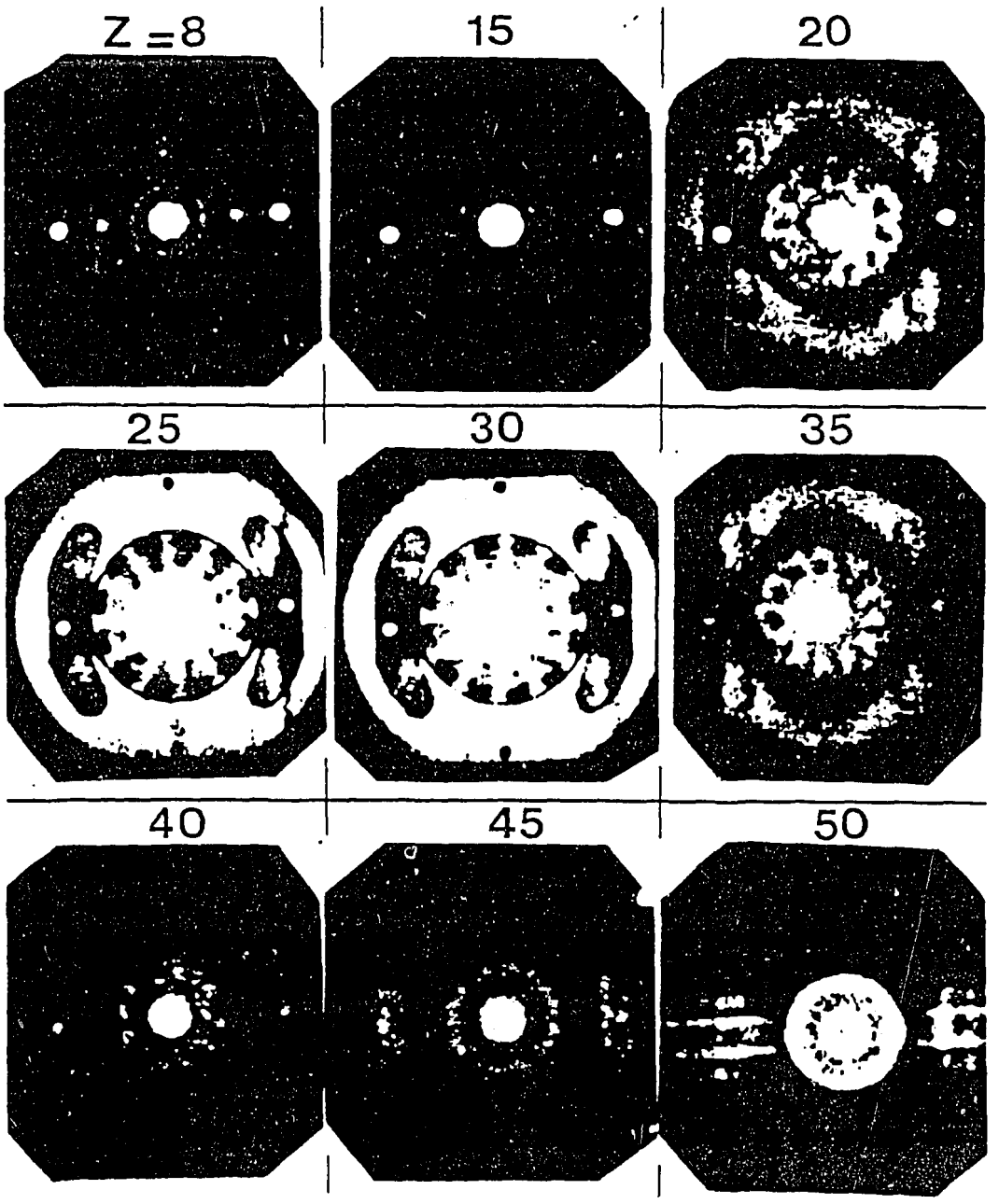

Fig. 1 - N.S.R. radiography of an electric motor. Longitudinal position (Z coordinate) of these transverse slices (planes X-Y) is given by the numbers.

giving a voxel of 1 mm³. For an irradiation time of two hours, 32 millions of scattered events are collected giving a density of about 50 events per mm³. The longitudinal position (Z) of the transverse slices (planes X-Y) is indicated by numbers on Fig. 1. On Z=8 slice, one can see the seven balls of the gear bearing the motor axis. On Z= 25 and Z=30 slices, the 0.6 mm gap between stator and rotor appears nicely. Z=50 slice is at the level of the motor collector. With this motor running, we did also a first application of R.D.N. to cineradiography. One can synchronize with some microseconds precision, the acquisition of the scattered events with an external signal phase-locked on the position of the running motor axis. The visualization matrix M(X,Y,Z) becomes a 4-D matrix M(X,Y,Z,T) where T is the time measured by the external synchronization signal. Because the total dimension of the mass memory is fixed, we have to decrease X,Y,Z dimensions to leave place to T. In our particular application, because the high level of symmetry of the rotor (12 blades), T dimension is height (120). The matrix M(X,Y,Z,T) has respective dimensions 40 , 40 , 10 , 120 with $\Delta X = \Delta Y = 1.27$ mm, $\Delta Z = 5.08$ mm and $\Delta T =$ 280 µs. So the field of radiography is reduced to the rotor and the edges of the stator. The motor was running at 1800 revolutions per minute and we needed nine hours to get about 50 events per matrix element of 8.2 mm³ - 280 µs. Despite this very long time, we were able to follow clearly the moving blades of the rotor.

III. Radiography of a human head

To illustrate the capability of N.S.R. in medical applications, Fig. 2 shows some radiographs obtained on a human head fixed in a formalin solution. Position of the head is so that the transverse planes X-Y correspond to sagittal slices. The visualization matrix M(X,Y,Z) has dimensions 160 × 160 × 80 respectively and $\Delta X = \Delta Y = 0.635$ mm, $\Delta Z = 2.54$ mm. On Fig. 2, four adjacent slices X-Y are summed giving a voxel of 4 mm³. For an irradiation time of one hour, 25 millions of scattered events are collected giving a density of about 10 events per mm³. The delivered dose is about 0.1 - 0.2 rad. The longitudinal position (TR) of the sagittal slices is indicated by numbers on Fig. 2. TR 31-34 corresponds to the median sagittal plane of the head. To facilitate the interpretation of these radiographs, Fig. 3 shows two comparable anatomical slices. The left-one compares with the TR 27-30) proton radiography, the right one with TR 31-34. Many details appear clearly on

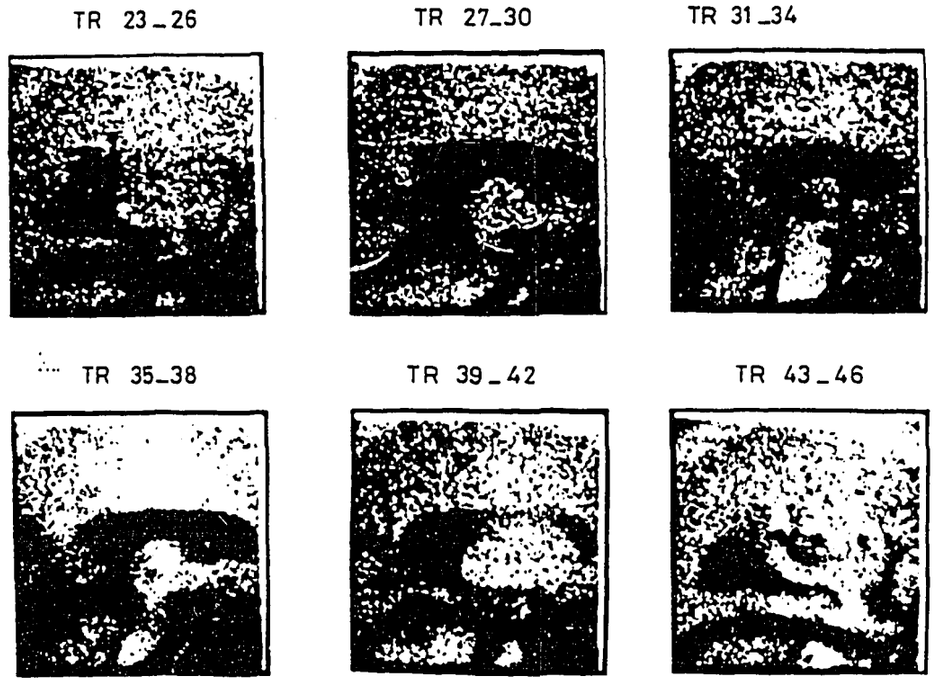

Fig. 2 - N.S.R. radiography of a human head. Successive sagittal slices of 1.1 cm width. Slice TR 31-34 corresponds to the median sagittal plane of the head.

Fig. 3 - Anatomical sagittal slices of a human head. The one on the left size compares with the proton radiography TR 27-30, the one on the right with TR 31-34.

the N.S.R. results and it shows that the volumic resolution of the method estimated about 6 mm^3 is satisfactory.

Perspectives of N.S.R.

These results are encouraging on the usefulness of the N.S.R. method but its use will be limited by the need of a big accelerator delivering a GeV proton-beam. But one has to point out that the very low intensity proton beam needed does not disturb the physic experiments of existing accelerators. The example of neutronography using neutron reactor for technical applications shows that N.S.R. could have in the future some development. Right now, N.S.R. is not of practical use because the irradiation time is much too long. Most of our work is to make radiographs faster. In 1977, we were able to treat 2 millions events per day,[6] in 1978 32 millions per day[3] and now 25 millions per hour. This is not enough and we have to increase our speed acquisition by at least a factor ten. Two limitations appear :

The first one is the computing time (50 µs) of the vertex interaction. We have now set a big buffer in front of the S.A.R. which allows to compute vertices permanently. So very soon, it will be possible to increase our speed acquisition by a factor 2-3. Furthermore, a new version of SAR will increase this speed by a factor ten in two years.

A second limit is due to the intensity of the incident beam crossing the localization chambers. Now, this intensity is of the order 2-4 × 10^5 protons per burst and to radiography 10 times faster, it has to be of the order 2-4 millions which is too much for the 1 m^2 chambers. So we plan to set four chambers, parallel to the beam on the left and right side to localize the scattered trajectories. In that way, we will be able to treat intense beams and obtain radiography in some minutes. This new set-up could be ready in two years.

References

1. J. Saudinos, G. Charpak, F. Sauli, D. Townsend, J. Vinciarelli, Nuclear scattering applied to radiography, Phys. Med. Biol. 20 (1975) 890.
2. G. Charpak, S. Majewski, Y. Perrin, J. Saudinos, F. Sauli, D. Townsend, J. Vinciarelli, Further results in nuclear scattering radiography, Phys. Med. Biol. 21 (1976) 941.
3. J.C. Duchazeaubeneix, J.C. Faivre, D. Garreta, B. Guillerminet, M. Rouger, J. Saudinos, P. Palmieri, C. Raybaud, G. Salamon, G. Charpak, G. Melchart, Y. Perrin, J.C. Santiard, F. Sauli, Nuclear scattering radiography, J. Comput. Assist. Tomogr., 4 (1980) 803.
4. B. Bricaud, J.C. Faivre, J. Pain, IEEE Trans. Nucl. Sci. NS26 (1979) 4641.
5. J.C. Duchazeaubeneix, Radiographie par diffusion nucléaire de protons d'énergie intermédiaire, Thèse d'Université, Université Paris-Sud, Centre d'Orsay (1982).
6. J.C. Duchazeaubeneix, J.C. Faivre, D. Garreta, B. Guillerminet, D. Legrand, M. Rouger, J. Saudinos, J. Berger, Nuclear scattering radiography of heavy materials, Materials Evaluation 37 (1979) 76.